

# **Discovery and validation of small molecule TIGIT inhibitors for cancer immunotherapy**

Yiwei Liang

Princeton International School of Mathematics and Science  
NJ, USA

Mentor: Dr. Moustafa Gabr

Cornell University  
NY, USA

## Abstract

Immunotherapy is an advanced method of cancer treatment. Immune checkpoint inhibition, using small molecule inhibitors to impede the functioning of immune checkpoints, is a common strategy applied in immunotherapy. T cell immunoreceptor with immunoglobulin and ITIM domain (TIGIT) is an immune checkpoint that impedes T cell functioning against tumor cells. This research focuses on finding suitable small molecules for TIGIT inhibition, thereby enhancing the immune system's defense against cancer cells. In the beginning, the binding sites on TIGIT were identified. TIGIT/CD112 and TIGIT/CD155 pharmacophore models were then used for virtual screening to identify potential small molecule TIGIT binders. The energy of interactions was further estimated by molecular docking using SwissDock, and the small molecules with more favorable interaction with TIGIT were advanced to further screening. Microscale thermophoresis was performed to validate physical interaction of the small molecules with TIGIT. Subsequently, AlphaLISA and the Promega blockade bioassay were applied to examine whether the small molecules could inhibit TIGIT/CD112 or TIGIT/CD155 interaction. Herein, one small molecule was successfully identified and validated to be useful for TIGIT inhibition in both cell-free and cell-based assays. This promising result sets the stage for future in vivo testing, in which the effectiveness of TIGIT inhibition in suppressing mice tumor growth will be evaluated.

**Keywords:** TIGIT, immune checkpoint inhibitor, immunotherapy, cancer, small molecule

## TABLE OF CONTENT:

<b>ABSTRACT.....</b>	<b>2</b>
<b>INTRODUCTION .....</b>	<b>3</b>
<b>METHODS .....</b>	<b>5</b>
DoGSiteScorer.....	5
FTSite.....	5
PrankWeb.....	5
Pharmacophore query.....	5
Virtual Screening Using Pharmacophore.....	5
Molecular Docking.....	6
Drug Properties Prediction by SwissADME and Druglikeness Evaluation Using the Lipinski's Rule.....	6
Microscale Thermophoresis (MST).....	6
AlphaLISA.....	7
HDock.....	7
Promega Blockade Bioassay.....	8
<b>RESULTS &amp; DISCUSSION.....</b>	<b>8</b>
Determination of Binding Sites on TIGIT.....	8
Using the Interaction of TIGIT with Other Proteins to Target Possible Binding Small Molecules to TIGIT.....	9
Identification of Possible Binding Molecules Using the Structure of Interaction Between TIGIT and CD112.....	9
Investigation on the Binding Affinity of TIGIT with CD155 and CD112.....	13
Identification of Possible Binding Molecules Using the Structure of Interaction Between TIGIT and CD155.....	14

<b>Future Research.....</b>	<b>18</b>
<b>CONCLUSION.....</b>	<b>18</b>
<b>ACKNOWLEDGEMENTS.....</b>	<b>18</b>
<b>REFERENCES .....</b>	<b>19</b>

## 1. Introduction

Cancer is one of the most severe and intimidating diseases of the 20th and 21st centuries [1]. Cancer has caught great attention in the past few decades, and its incidence has increased dramatically [1]. Between 2010 to 2019, global cancer incidence increased by 26%, and global cancer death increased by 21% [2]. It is the second leading cause of death globally, with about 9.9 million deaths in 2020 [2]. In 2023, about 1.96 million new cancer cases and 610 thousand cancer deaths are predicted to occur in the United States [3]. As cancer has become one of the most fatal diseases around the globe, cancer therapy remains a challenge and has become an important focus in modern science.

Cancer stems from normal human cells that have transformed into tumor cells [4]. Unlike benign tumors, cancerous tumors develop toward other body parts and invade other organs [5]. There are currently more than 100 known cancer types, with the most common being lung, breast, and colorectal cancer [6]. The specific reason cancer damages the body varies between cancer types. However, the general mechanism is that cancer cells destroy normal body cells, block nutrient or oxygen supply, and allow waste to build up in the body [7].

Various methods for curing cancer have been developed. Primary treatments include surgery, radiation therapy, chemotherapy, and immunotherapy [8]. The first three treatments (surgery, radiation therapy, chemotherapy) are traditional methods used for cancer therapy. However, these treatments contain multiple side effects. For surgical treatment, one of the earliest forms of cancer treatment, complete treatment of cancer is challenging, and only localized tumors may be entirely removed [8]. Unremoved cancer cells can regrow into new tumors and spread to other parts of the body [8]. Radiation therapy uses high-energy radiation to eliminate cancer cells' ability to divide and replicate, eventually killing cancer cells [9]. However, radiation therapy may damage healthy tissues, causing skin rashes and inflammation. More than 77% of patients reported experiencing acute toxicity of grade 3 or higher after receiving radiation therapy [10]. Chemotherapy, which uses cytotoxic chemicals to kill the tumor, might damage healthy cells and frequently fail to work [11]. On the other hand, immunotherapy utilizes the immune system to treat cancer. It is a novel approach that does not contain acute side effects and is relatively safe compared to other therapies since it uses the body's immune system to fight against cancer [12].

The key mechanism of immunotherapy is to stimulate the immune system, allowing the immune system to attack cancer cells and tumor tissues [12]. Immunotherapy first developed in the 19<sup>th</sup> century, when Dr. William Coley used bacterial toxins against cancer patients, triggering anti-tumor responses in some patients [13]. However, it was not until the 1960s that T cells were recognized for their significant role in anti-tumor immune responses, followed by the increasing use of T cell growth factor interleukin-2 (IL-2) [13]. Currently, two major types of immunotherapies exist: cellular immunotherapy for tumors and immune checkpoint inhibition [14]. Immunotherapy has grown to become a powerful method in cancer treatment. The number of approved immunotherapy drugs and successful clinical cases has increased dramatically since the 21<sup>st</sup> century [15].

Immune checkpoints are part of the immune system. They are located on T cells' surface and serve as immune system regulators [12]. Immune checkpoints reduce the excessive inflammation of the body [12]. They are an exceedingly vital part of the body, without them, the immune system will react perpetually, killing the human body. However, tumors hijack the inhibitory response to prevent the attack of T cells and hinder anti-

tumor immune responses [12]. Immune checkpoint inhibitors work by lowering the activity of immune checkpoints, activating T cells, and allowing the immune system to attack tumor tissues further [16]. Previous research on immune checkpoint inhibition mainly deals with two immune checkpoints, cytotoxic T lymphocyte-associated protein 4 (CTLA-4) and programmed cell death protein 1 / programmed cell death ligand-1 (PD-1/PD-L1) [17]. Both have shown promising progress and results in clinical trials [18]. PD-1 inhibitors are more commonly investigated [18]. PD-1 inhibitors can increase T cell activity and obstruct tumor growth simultaneously [19]. PD-1 inhibitors have been used in lung, head, neck, and kidney cancer, while CTLA-4 inhibitors are mainly used in severe melanoma [19]. By 2018, four drugs regarding immune checkpoint inhibition had been approved by the Food and Drug Administration (FDA) against various types of cancer [12].

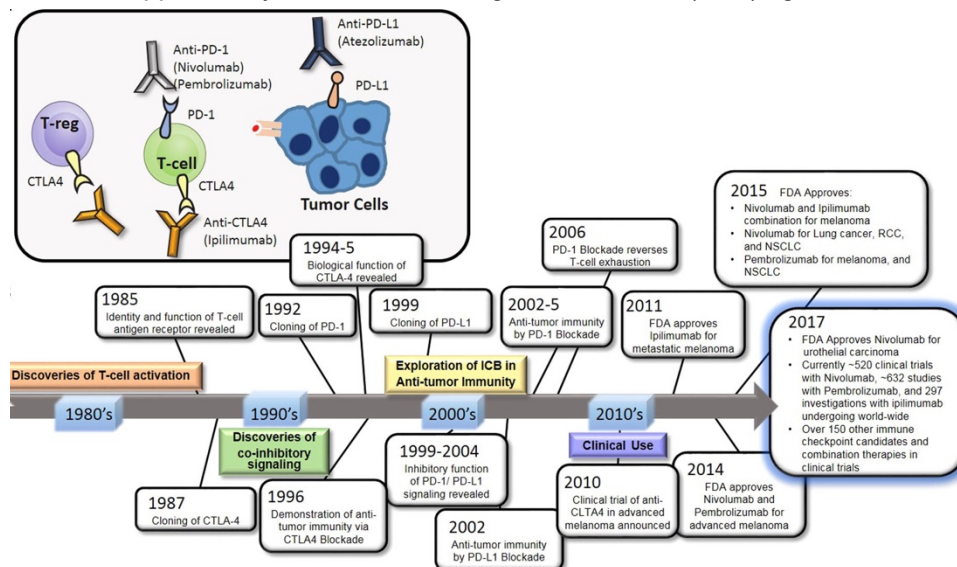


**Figure 1.** Timeline for the development of immune checkpoint inhibition therapy since the 1980s [12].

receptor-related 2 (PVRL2, nectin-2, or CD112) [20]. CD155 is present in both healthy tissues and tumors, as well as antigen-presenting cells (APCs) in tumor microenvironment (TME) [22]. Its large presence on tumor cells facilitates tumor growth and the spread of tumor cells [23]. For example, PVRL1 (nectin-1 or CD111) promotes TIGIT-mediated T cell deactivation by stabilizing the CD155 present in tumor cells. The depletion of PVRL1 stimulates T cells' activation and reduces tumor cell growth [21]. Studies have further shown that inhibition of CTLA-4 and PD-1 only triggers activation of T cells, while inhibition of TIGIT encourages the immune responses of both NK cells and T cells, a unique property among other immune checkpoints [24]. Blockage of TIGIT reverses the exhaustion of anti-tumor NK cells and decelerates tumor growth, extending the host's survival in vivo [24]. With these essential properties, targeting TIGIT and finding its inhibitors is a promising and critical strategy in cancer immunotherapy. However, more research on TIGIT inhibition needs to be performed. The field of TIGIT inhibition is little explored but beholds extensive value.

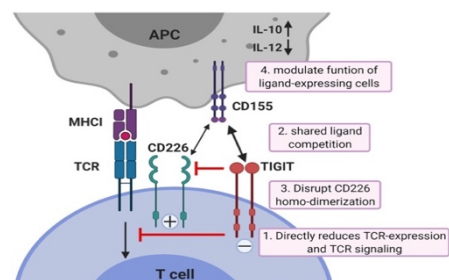


**Figure 2.** Mechanisms of TIGIT inhibition of T cells [21].

T cell immune receptor with immunoglobulin and ITIM domain (TIGIT) is an immune checkpoint expressed on both T cells and natural killer (NK) cells [20]. TIGIT hinders T cell activation by inducing interleukin 10 (IL-10) production by dendritic cells and prevents the immune system from attacking the tumor tissue [21]. TIGIT binds to both poliovirus receptor (PVR or CD155) and poliovirus

In this research, computational approaches are used to search for small molecules that successfully inhibit TIGIT against CD112 and CD155 interactions. In the first experiment, binding sites on TIGIT are identified to ensure binding is possible. In the second experiment, by identifying the binding sites between TIGIT and CD112 or CD155, molecules that share common binding sites and are potential binding ligands to TIGIT are collected. In the third experiment, the binding free energies are estimated, and molecules with the highest binding affinities

to TIGIT are selected. The molecules' drug-likeness is then examined, choosing druggable molecules. Lastly, the selected molecules are purchased, and experiments using MST, AlphaLISA, and the Promega blockade bioassay are performed to determine whether the molecules successfully bind to TIGIT and can inhibit the interaction between TIGIT and CD112 or CD155.

## 2. Methods

### 2.1 DoGSiteScorer

There are four primary methods to identify binding sites in proteins: the geometric method, the energetic-based method, the machine learning method, and the template-based method. In this research, the first three methods are used to identify binding sites on TIGIT.

DoGSiteScorer (<https://proteins.plus/>) uses the geometric method to identify potential binding sites on a protein [25]. Geometric methods rely on detecting the size of binding sites. Thus, DoGSiteScorer is a grind-based approach solely based on the 3D structure of the protein. When the results are presented, the volume surface area and drug score will also be calculated.

By entering the PDB-Code in the search box on ProteinPlus and pressing "Go", the website displays the targeted protein's 3D structure, and various available functions will be introduced on the right. Select "DoGSiteScorer" and fill in the settings, then press "Calculate" to identify the potential binding sites.

### 2.2 FT Site

The premise behind the energy-based method FT Site [26] is the experimental evidence that binding sites bind with small molecules with different polarities. FT Site is available at <https://ftsite.bu.edu/>.

After entering the name of the protein, PDB ID, and email address, press "Find My Binding Site" to begin search.

### 2.3 PrankWeb

PrankWeb (<https://prankweb.cz/>) is a novel resource providing interface to P2Rank, a type of machine learning method to identify binding sites [27]. PrankWeb is based on the prediction of local chemical neighborhood ligandability centered on the protein surface.

After entering the PDB code on PrankWeb and changing the default settings, select "Submit" to predict the binding sites.

### 2.4 Pharmacophore query

PocketQuery (<http://pocketquery.csb.pitt.edu/>) is a web interface aimed to explore the interactions between different proteins and binding sites [28]. By using PDB codes, which represent protein-protein interaction molecular models, PocketQuery identifies the druggable clusters on each chain of the structure. The results include size, maximum cluster distance (Dist), FastContact energy ( $\Delta G$ ), rosetta energy ( $\Delta\Delta G$ ), absolute change in solvent accessible surface area ( $\Delta SASA$ ), relative  $\Delta SASA$ , and cluster score [29].

On the PocketQuery website, enter the PDB ID and select "Search", the results will be shown on the right side. Double click "Score" on the top right corner, and the results will be displayed from highest cluster score to lowest cluster score.

### 2.5 Virtual Screening Using Pharmacophore

ZINCPharmer (<http://zincpharmer.csb.pitt.edu/>) is an online pharmacophore search software. By using the

clusters from PocketQuery and selecting certain pharmacophore classes, ZINCPharmer screens for small molecules that contain similar structures from the ZINC database using the Pharmer open-source pharmacophore search technology [30].

After selecting the top five scoring designated clusters, press “Export” and select “Send to ZINCPharmer.” Then, press “Viewer” and turn down the “Receptor Residues.” Zoom in to have a closer look at the cluster. Select three criteria under “Pharmacophore” and press “Submit Query.” Rank the results from lowest to highest RMSD. Choose the three results with the lowest RMSD.

## 2.6 Molecular Docking

Swissdock (<http://www.swissdock.ch/docking>) is an online platform that provides docking for small molecules against target proteins. Swissdock uses theoretical methods to calculate the energy of interaction between small molecules and proteins. It uses the EADock DSS engine to operate [31]. All calculations are done by the server. The docking data, the target protein structures, and the ligands are presented [31].

Submit the target protein in the “Target selection” by searching it with the protein’s URL and PDB code or uploading a mol2 standard protein file. Submit the “Ligand selection” by searching the ZINC AC or uploading a mol2 standard ligand file. Then, enter the project’s name and user email to receive the notification when the result comes out. Press “Start Docking” to begin the molecular docking. Several hours are needed for the calculation.

## 2.7 Drug Properties Prediction by SwissADME and Druglikeness Evaluation Using the Lipinski’s Rule

The SwissADME (<http://www.swissadme.ch/>) platform is used to predict the properties of drug compounds. Chemical properties, drug-likeness, pharmacokinetics, and detailed information such as molecular mass, number of hydrogen bonds, and water solubility are provided [32].

Collect SMILES from ZINC 12 (<https://zinc12.docking.org/>) by entering the ZINC ID of the molecule in the “Quick Search Bar.” Then submit SMILES into the “Enter a list of SMILES here:” section on SwissADME. Click “Run” to begin the search. A detailed depiction of the molecule will be provided. Features such as molecular weight, lipophilicity, hydrogen donor count, and hydrogen acceptor count are essential for determining the druggability of the compound.

Lipinski’s rule is further applied to estimate if a molecule is druggable. Lipinski’s rule has four standards: the target molecule should have a molar mass of less than 500 Dalton (g/mol), less than five hydrogen bond donors, less than ten hydrogen bond acceptors, and a calculated LogP value of less than five. These standards help evaluate if a molecule has good absorption and permeation as a drug.

## 2.8 Microscale Thermophoresis (MST)

There are multiple methods to detect protein-small molecule interactions. Common approaches to investigate protein–small molecule interactions include Surface Plasmon Resonance (SPR), Isothermal Titration Calorimetry (ITC), and Microscale Thermophoresis (MST). SPR measures the change in the local refractive index near the surface of a thin metal sheet [33], ITC examines the heat change during a binding interaction [34], and MST detects the change in molecular movement in a temperature gradient before and after binding [35]. MST is a free solution method that works in standard buffers and biological liquids. This research adopts MST to test whether the selected druggable small molecule will successfully bind to TIGIT.

Monolith NT.115 instrument from NanoTemper is used to assess the compounds/TIGIT interaction. His-tagged human TIGIT is purchased from SinoBiological and is labeled with His-tag Labeling Kit RED-tris-NTA

2nd Generation from NanoTemper (Cat #MO-L018). TIGIT is dissolved in PBS buffer (pH 7.4) with 0.1% bovine serum albumin (BSA) and 0.05% Tween 20. The concentration of the fluorescently labeled TIGIT is kept constant at 50 nM. A volume of 5  $\mu\text{L}$  of the corresponding samples is filled in MST capillaries with a final DMSO concentration of 2%. Subsequently, the samples within the capillaries are incubated for 20 min at room temperature prior to the measurements. Changes in thermophoretic properties are recorded as changes in fluorescence intensity against various concentrations of the tested compounds with fluorescently labeled TIGIT. Normalized changes in fluorescence ( $F_{\text{norm}}$ ) against the compound concentration are plotted to obtain dose-response curves.  $F_{\text{norm}}$  is the ratio of fluorescence measured before and during thermophoresis. A continuous change in  $F_{\text{norm}}$  as the concentration of the small molecule increases indicates successful binding between the protein and small molecule. The experiment is performed in triplicates in three independent runs.

## 2.9 AlphaLISA

AlphaLISA is a method used to evaluate the ability of small molecules to inhibit protein-protein interaction. The mechanism of AlphaLISA is based on the donor bead's ability to produce singlet oxygen under laser irradiation and to trigger chemiluminescent emission in the acceptor bead [36]. If inhibition is successful, the donor and acceptor would be too far away for luminescence to occur, and the activity will decrease as the concentration of the inhibitor increases.

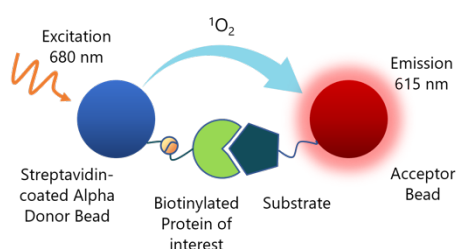


**Figure 3.** Mechanism of AlphaLISA [36].

Percent activity is a measurement of fluorescent intensity. The experiment is performed in triplicates in three independent runs.

**Table 1.** The amount of solution added to each well [37].

	Blank	Positive Control	Test Inhibitor
3x Immuno Buffer 1	2 $\mu\text{L}$	2 $\mu\text{L}$	2 $\mu\text{L}$
CD112-His (5 ng/ $\mu\text{L}$ )	2 $\mu\text{L}$	2 $\mu\text{L}$	2 $\mu\text{L}$
Distilled Water	2 $\mu\text{L}$	2 $\mu\text{L}$	2 $\mu\text{L}$
Test Inhibitor	-	-	2 $\mu\text{L}$
Inhibitor Buffer (no inhibitor)	2 $\mu\text{L}$	2 $\mu\text{L}$	-
1x Immuno Buffer 1	2 $\mu\text{L}$	-	-
TIGIT-biotin (4 ng/ $\mu\text{L}$ )	-	2 $\mu\text{L}$	2 $\mu\text{L}$
<b>Total</b>	<b>10 <math>\mu\text{L}</math></b>	<b>10 <math>\mu\text{L}</math></b>	<b>10 <math>\mu\text{L}</math></b>

## 2.10 HDOCK

HDOCK (<http://hdock.phys.hust.edu.cn/>) is a server designed to investigate protein-protein docking [38]. The interaction of the proteins is estimated using a hybrid algorithm of template-based and template-free docking [38]. The results include docking score, confidence score, ligand RMSD ( $\text{\AA}$ ), and interface residues. Binding models are ranked based on their docking score. The scores are relative and do not represent the true binding affinity [38]. A more negative docking score indicates a more favorable interaction.

To start the docking process, provide the receptor molecule in the “input receptor molecule” section and the ligand molecule in the “input ligand molecule” section by using one of the four options on the website. Press “submit” to start docking.

## 2.11 Promega Blockade Bioassay

The Promega blockade bioassay measures the inhibition strength of small molecules against target immune checkpoints in a cell-based environment [39]. The TIGIT/CD155 blockade bioassay contains TIGIT effector cells and CD155 aAPC/CHO-K1 cells. The TIGIT effector cell contains TIGIT and a luciferase reporter, which can respond to both T cell receptor activation and CD226 co-stimulation [39]. By co-culturing the two cell types, TIGIT inhibits CD226 activated luminescence [39]. When an inhibitor is added, the ability of TIGIT to prevent CD226 activation is inhibited, promoting luminescence.

Prepare the TIGIT effector cell, CD155 aAPC/CHO-K1 cell, and test small molecules by following the TIGIT/CD155 blockade bioassay technical manual. After preparation, 120  $\mu\text{L}$  of TIGIT effector cells are added to each well and incubated overnight in a 37°C, 5%  $\text{CO}_2$  incubator. Subsequently, add 20  $\mu\text{L}$  of tested small molecules with different concentrations and 20  $\mu\text{L}$  of CD155 aAPC/CHO-K1 cells to each well. The mixture is incubated at 37°C for six hours. 120  $\mu\text{L}$  of Bio-Glo™ reagent is then added to each plate and incubated for 5-10 minutes. Results are measured using a luminometer.

## 3. Results & Discussion

### 3.1 Determination of Binding Sites on TIGIT

Using the following three means to identify potential binding sites on TIGIT ensures that small molecules can bind to TIGIT.

#### 3.1.1 DoGSiteScorer

Protein Plus DoGSiteScorer identified three possible binding sites on the chains A and B of TIGIT (Table 2 and Figure 4), one on chain A and two on chain B. Three properties of the binding sites are provided: the volume, surface area, and drug score. The largest binding site is P\_0 on chain B, represented in yellow on the right-hand figure in Figure 4. It has a volume of 170.43  $\text{\AA}^3$  and a surface area of 326.7  $\text{\AA}^2$ . It also has the highest drug score, 0.49. All of these data make P\_0 on chain B the most druggable binding site on chains A and B of TIGIT.

**Table 2.** The three binding sites on chain A & B predicted by DoGSiteScorer.

Name	Volume ( $\text{\AA}^3$ )	Surface ( $\text{\AA}^2$ )	Drug Score
P_0 (Chain A)	166.91	273.12	0.28
P_0 (Chain B)	170.43	326.7	0.49
P_1 (Chain B)	135.04	224.6	0.00

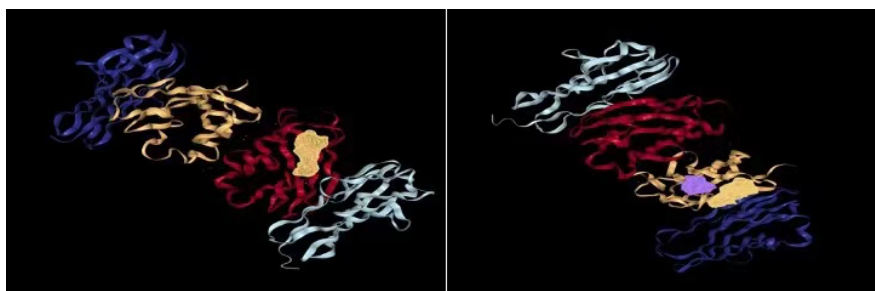




**Figure 4.** DoGSiteScorer predicted binding sites on chain A (left) and chain B (right) of TIGIT (represented in yellow & purple).

### 3.1.2 FT Site

Three binding sites are detected using FT site, represented in purple, blue and green in Figure 5.

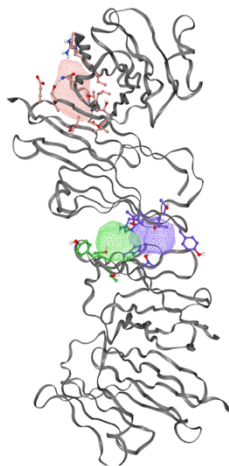


**Figure 5.** FT site predicted binding sites (represented in pink, purple & green).

### 3.1.3 PrankWeb

Two binding sites are predicted by PrankWeb. The pocket with the highest pocket score (4.61) and probability score (0.212) is pocket 1, represented in blue in Figure 6.

**Table 3.** Two binding sites predicted by PrankWeb on TIGIT.

Pocket	Pocket Score	Probability score	AA Count
1	4.61	0.212	16
2	4.52	0.207	13

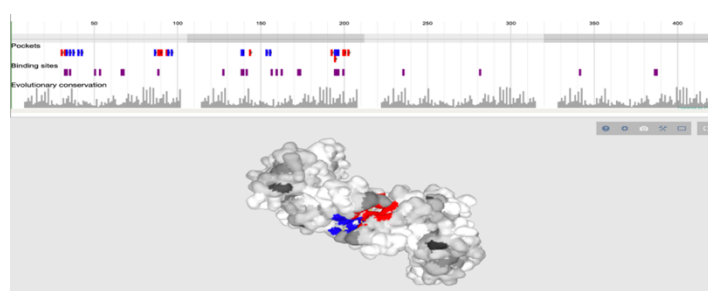


**Figure 6.** PrankWeb predicted binding sites (represented in blue & red).

All three methods indicated possible binding sites on TIGIT, ensuring that binding to TIGIT is feasible. The following experiment searches for small molecules that contain specific structures that allow binding to TIGIT.

## 3.2 Using the Interaction of TIGIT with Other Proteins to Target Possible Binding Small Molecules to TIGIT

### 3.2.1 Identification of Possible Binding Molecules Using the Structure of Interaction Between TIGIT and CD112

The pharmacophore of CD112 and CD155 is crucial in the search for binding molecules to TIGIT [40]. Since most clinical trials focus on TIGIT/CD112 interaction, with PocketQuery, the pharmacophore model (PDB code: 5V52) of CD112 binding to TIGIT is identified first. Virtual screening is then used to search for molecules that possess such features.

### 3.2.1.1 PocketQuery

The top five highest-scoring results of PocketQuery are listed. Scoring differentiates the druggability of the clusters. A higher score indicates the cluster has a higher affinity and matching to the binding sites on TIGIT. Cluster 1 has the highest score 0.831758, the highest Av  $\Delta G^{FC}$  -3.64 (absolute value), and the highest Av  $\Delta SASA$  127.16. The five clusters are then used to perform virtual screening.

**Table 4.** Top five clusters with scoring from PocketQuery (CD112).

Cluster	Residue	Ch	Sz	Dist	Av $\Delta G^{FC}$	Av $\Delta \Delta G^R$	Av $\Delta SASA$	Av $\Delta SASA\%$	Score
1	PHE145	D	1	0	-3.64	2.156	127.16	77.5	0.831758
2	PHE145; LEU67	D	2	11.1451	-2.96	1.8113	93.345	59.85	0.747289
3	PHE145; LEU67; TYR64	D	3	11.1451	-2.11667	1.31003	76.6867	48.0667	0.708706
4	MET89	D	1	0	-1.27	0.3188	73.5	47	0.696018
5	PHE145; LEU67; TYR64; GLY148	D	4	11.1451	-1.62	1.30465	64.495	57.65	0.695621

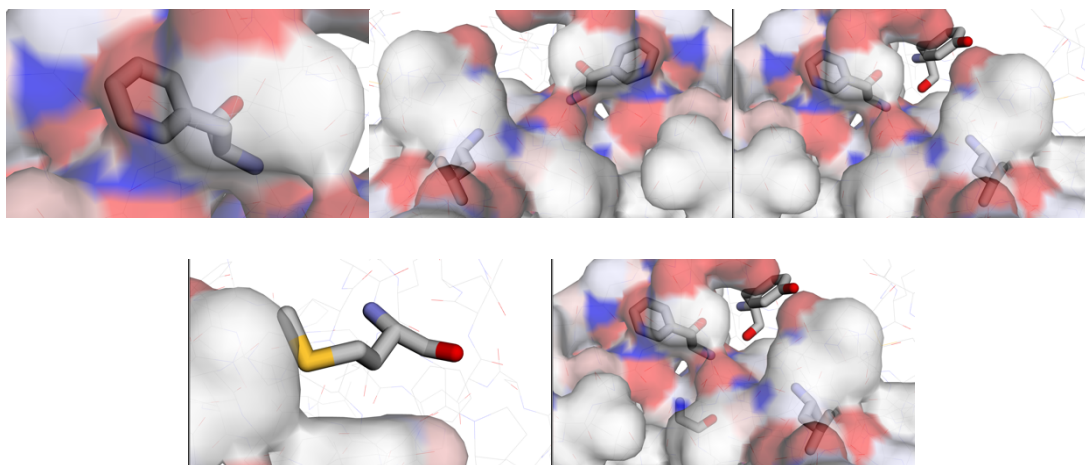


**Figure 7.** Molecular structure for top five scoring clusters from PocketQuery.

### 3.2.1.2 Virtual Screening

By applying virtual screening using ZINCPharmer, the three lowest RMSD (Root-mean-square deviation of atomic positions) results from each cluster are presented in Table 5, which gives a total of fifteen molecules. A lower RMSD indicates a better matching between the molecules and the clusters.

**Table 5.** Results for top three molecules from each cluster (total of 15) with lowest RMSD from ZINCPharmer.

Cluster	Pharmacophore Class	x	y	z	Radius	Name	RMSD	Mass
1	Hydrophobic	-0.38	17.37	-44.06	1.00	ZINC77785621	0.000	324
	Aromatic	-0.38	17.37	-44.06	1.10	ZINC36225700	0.000	292
	Hydrogen Donor	3.52	14.88	-46.44	0.50	ZINC72262118	0.000	437

2	Hydrophobic	-0.38	17.37	-44.06	1.00	ZINC00628285	0.000	502
	Aromatic	-0.38	17.37	-44.06	1.10	ZINC40255765	0.000	482
	Hydrophobic	10.56	10.20	-39.21	1.00	ZINC40192954	0.000	480
3	Hydrophobic	-0.38	17.37	-44.06	1.00	ZINC70678006	0.000	383
	Hydrogen Donor	5.71	18.45	-47.94	0.50	ZINC93468196	0.000	354
	Hydrogen Acceptor	5.71	18.45	-47.94	0.50	ZINC93468121	0.000	289
4	Hydrogen Acceptor	18.54	15.79	-35.11	0.50	ZINC78252803	0.005	311
	Hydrogen Donor	15.42	17.41	-35.91	0.50	ZINC78252803	0.005	311
	Hydrophobic	12.82	16.32	-32.92	1.00	ZINC94486449	0.005	246
5	Hydrophobic	-0.38	17.37	-44.06	1.00	ZINC67909114	0.006	310
	Aromatic	7.58	19.23	-43.15	1.10	ZINC02456504	0.006	441
	Hydrogen Donor	5.71	18.45	-47.94	0.50	ZINC20190112	0.007	461

The fifteen small molecules selected have the highest matching with the five pharmacophores on CD112, which means these molecules have a higher possibility of binding to TIGIT. The following experiment will examine the affinity and thermodynamic data of the molecule's interaction with TIGIT.

### 3.2.1.3 Molecular Docking Results for TIGIT

The result of each compound's Swissdocking is presented in Table 6. The lowest binding energy of the compound with TIGIT is expressed using the estimated Gibbs free energy ( $\Delta G$ ). A more negative  $\Delta G$  means a more favorable interaction between TIGIT and the molecule. ZINC67909114 (-10.94), ZINC20190112 (-10.16), and ZINC00628285 (-9.60) are the top three molecules with the most negative  $\Delta G$ . These three molecules are more favorable in binding to TIGIT than other molecules.

**Table 6.** List of the Lowest Binding Free Energy from Swissdock.

Compound	Cluster	Full Fitness (kcal/mol)	Estimated $\Delta G$ (kcal/mol)
ZINC77785621	8	-2298.34	-7.67
ZINC36225700	0	-2260.77	-7.68
ZINC72262118	7	-2205.93	-8.52
ZINC00628285	1	-2202.06	-9.60
ZINC40255765	17	-2255.54	-7.83
ZINC40192954	3	-2259.50	-7.59
ZINC70678006	1	-2260.60	-7.89
ZINC93468196	4	-1948.68	-7.86
ZINC93468121	11	-2247.63	-7.11
ZINC78252803	14	-2203.04	-8.26
ZINC94486449	26	-2232.88	-7.26
ZINC67909114	7	-2207.16	-10.94
ZINC02456504	1	-2193.97	-7.68
ZINC20190112	13	-2260.55	-10.16

ZINC77785621	ZINC36225700	ZINC72262118	ZINC00628285	ZINC40255765
--------------	--------------	--------------	--------------	--------------

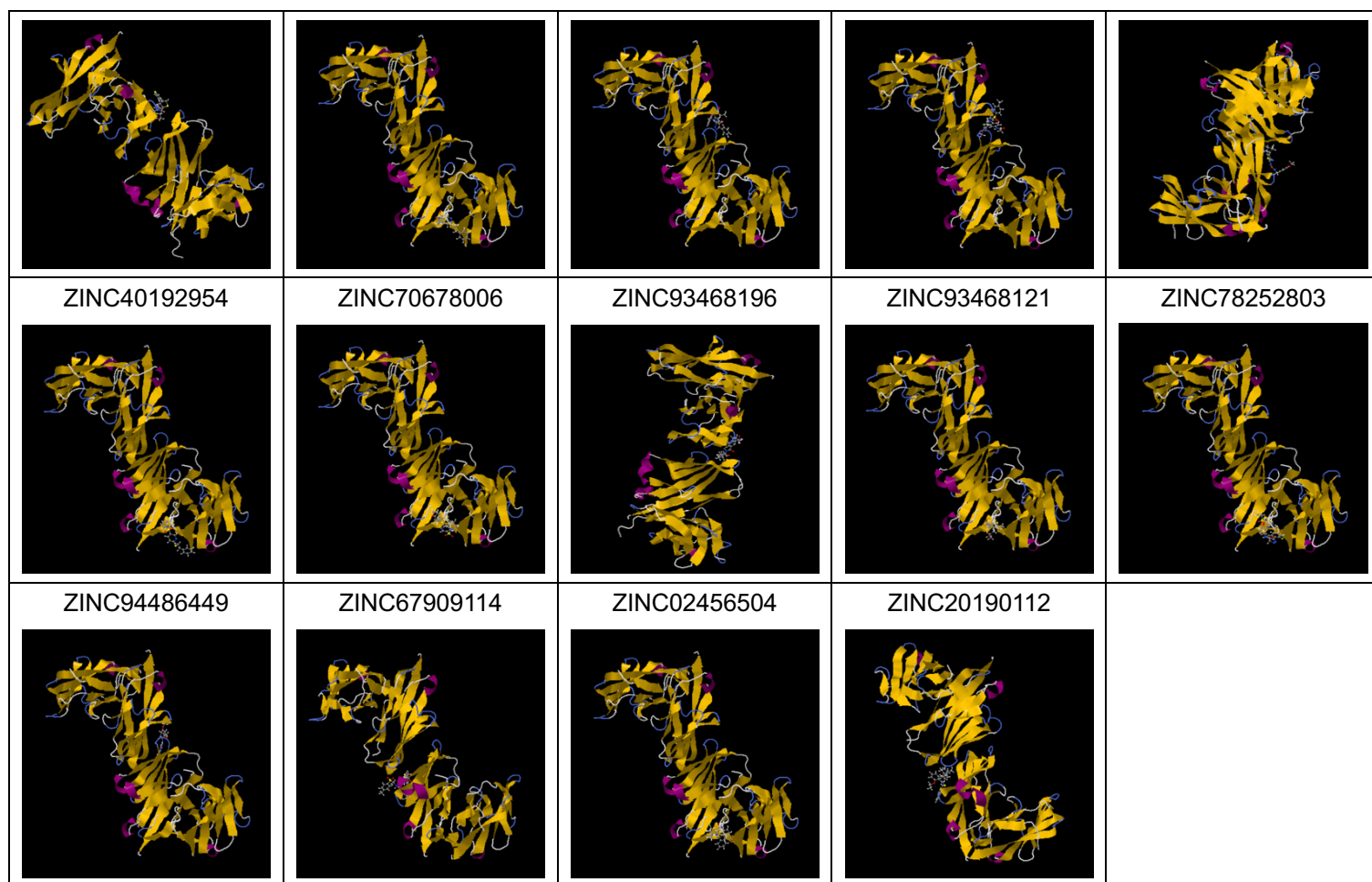


**Figure 8.** Molecular docking results of selected molecules from Swisdock.

The next experiment testifies the druglikeness of the three molecules with the highest binding affinity to TIGIT. The results help determine their possibility of being utilized as immune checkpoint inhibitors.

#### 3.2.1.4 Drug Properties Estimated by SwissADME

Among the three molecules (ZINC67909114, ZINC20190112, ZINC00628285), two of which (ZINC67909114, ZINC20190112) follow the Lipinski's rule. The two molecules are highly possible of drug utility.

**Table 7.** The druglikeness of the molecules.

	Number of hydrogen bond donors	Calculated LogP value	Molecular mass	Number of hydrogen bond acceptors	Druglikeness according to the Lipinski's rule
ZINC67909114	2	3.08	310.41	1	Yes
ZINC20190112	2	4.18	461.08	1	Yes
ZINC00628285	2	2.60	501.98	5	No

#### 3.2.1.5 Commercial Availability

The commercial availability of the two druggable molecules is investigated using the ZINC database. Only ZINC67909114 is commercially available. Thus, subsequent research proceeded with ZINC67909114.

#### 3.2.1.6 Detection of Protein-Small Molecule Interaction Using MST

By using microscale thermophoresis (MST), the result shows that as the concentration of ZINC67909114 increases, the percent normalized fluorescent intensity (%F<sub>norm</sub>) does not vary significantly. This indicates that

ZINC67909114 does not bind to TIGIT, and no TIGIT/ZINC67909114 interaction is present, even at high concentrations up to 30  $\mu\text{M}$ .

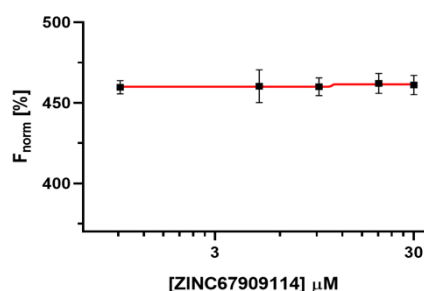


**Figure 9.** Monitoring fluorescence change using MST to assess the TIGIT binding affinity with ZINC67909114.

### 3.2.1.7 Investigation of ZINC67909114 on TIGIT Inhibition in a Cell-free Environment

By using AlphaLISA, the result indicates that as the concentration of ZINC67909114 increases, the percent activity remains constant. Therefore, ZINC67909114 fails to inhibit the interaction between TIGIT and CD112, even at high concentrations of up to 50  $\mu\text{M}$ .

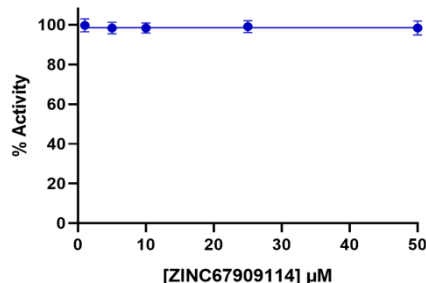


**Figure 10.** Using the change in percent activity from AlphaLISA to evaluate ZINC67909114 inhibition of TIGIT/CD112 interaction.

The two experiments show that ZINC67909114 fails to function as an inhibitor for TIGIT.

### 3.2.2 Investigation on the Binding Affinity of TIGIT with CD155 and CD112

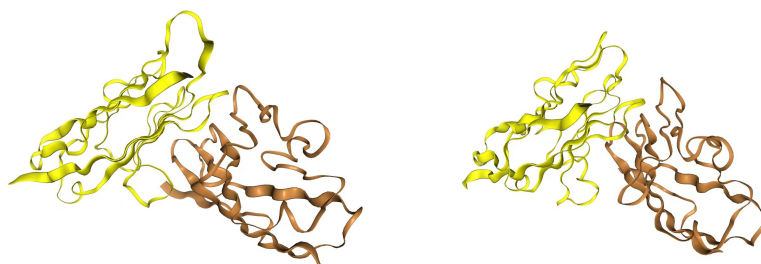
The failure of the previous approach indicates that using the structure of interaction between TIGIT and CD112 fails to identify small molecules for TIGIT inhibition. In subsequent research, another binding protein is needed to screen for potential inhibitors. CD155 is another binding protein to TIGIT. The pharmacophore model of TIGIT with CD155 should also be applicable in pharmacophore screening. HDock is used to estimate the relative binding affinity of TIGIT with CD155 and CD112. The results from HDock indicate that TIGIT has a higher binding affinity toward CD155 than CD112, as the interaction of different binding models of TIGIT to CD155 is more favorable than that of TIGIT to CD112. This means using the pharmacophore model of TIGIT/CD155 to screen for potential inhibitors should be more promising than using the pharmacophore model of TIGIT/CD112.

**Table 8.** Predicted Interaction Between TIGIT and CD112.

Rank	1	2	3	4	5	6	7	8	9	10
Docking Score	-331.64	-223.26	-220.01	-211.48	-210.52	-206.83	-205.56	-204.74	-201.59	-200.28
Confidence Score	0.9742	0.8123	0.8022	0.7737	0.7704	0.7571	0.7524	0.7493	0.7373	0.7322
Ligand rmsd (Å)	0.25	24.75	52.29	35.67	42.91	13.16	42.13	29.90	21.30	15.20

**Table 9.** Predicted Interaction Between TIGIT and CD155.

Rank	1	2	3	4	5	6	7	8	9	10
Docking Score	-352.65	-234.01	-231.57	-231.56	-225.52	-225.49	-222.33	-221.41	-220.70	-216.43
Confidence Score	0.9829	0.8429	0.8364	0.8363	0.8191	0.8190	0.8095	0.8066	0.8044	0.7906
Ligand rmsd (Å)	0.40	22.93	25.68	30.51	28.48	25.94	24.94	29.70	25.01	24.68

**Figure 11.** Binding model No. 1 of TIGIT with CD155 (left) and CD112 (right).

### 3.2.3 Identification of Possible Binding Molecules Using the Structure of Interaction Between TIGIT and CD155

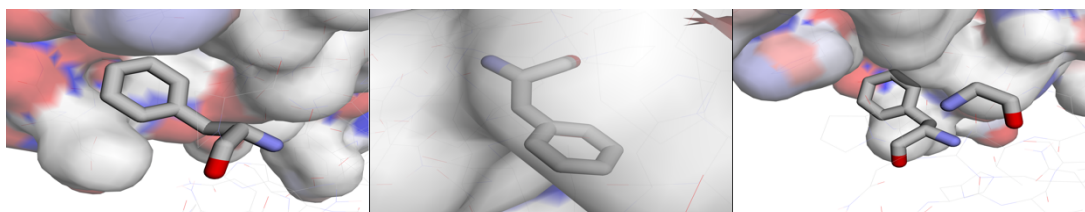
The pharmacophore model (PDB code: 3UDW) of TIGIT and CD155 binding will be used to search for potential inhibitors.

#### 3.2.3.1 PocketQuery

The top five scoring clusters are selected. The highest scoring cluster has a score of 0.850932, an Av  $\Delta G^{FC}$  of -3.58, and an Av  $\Delta SASA$  of 132.69.

**Table 10.** Top five clusters with scoring from PocketQuery (CD155).

Cluster	Residue	Ch	Sz	Dist	Av $\Delta G^{FC}$	Av $\Delta \Delta G^R$	Av $\Delta SASA$	Av $\Delta SASA\%$	Score
1	PHE128	C	1	0	-3.58	0.6484	132.69	80.9	0.850932
2	PHE128	D	1	0	-3.54	0	126.05	76.8	0.809682
3	PHE128; GLY131	C	2	6.3562	-1.7	0.8799	80.5	84.2	0.752957
4	PHE128; GLN63	C	2	11.7508	-1.325	0.79715	101.355	65.3	0.708548
5	PHE128; GLY131; GLN63	C	3	11.7508	-0.82333	0.9019	77.0067	72.7	0.700594





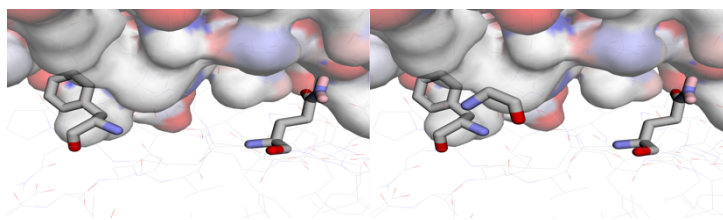


**Figure 12.** Molecular structure for top five clusters with scoring from PocketQuery.

### 3.2.3.2 Virtual Screening

Three pharmacophore classes are selected from each cluster to search for potential binding small molecules. Three molecules with the lowest RMSD are chosen from each cluster, and the fifteen molecules are listed in Table 11.

**Table 11.** Results for top three molecules from each cluster (total of 15) with lowest RMSD from ZINCPharmer.

Cluster	Pharmacophore Class	x	y	z	Radius	Name	RMSD	Mass
1	Hydrophobic	20.89	-37.91	14.90	1.00	ZINC11616526	0.000	302
	Hydrogen Acceptor	22.52	-39.16	9.10	0.50	ZINC03794711	0.000	220
	Hydrogen Donor	22.52	-39.16	9.10	0.50	ZINC02901892	0.000	249
2	Hydrophobic	-10.52	-32.37	31.91	1.00	ZINC00119434	0.000	335
	Aromatic	-10.52	-32.37	31.91	1.10	ZINC59187897	0.000	373
	Hydrogen Donor	-11.17	-29.83	36.37	0.50	ZINC77591929	0.000	370
3	Hydrophobic	22.04	-38.90	14.75	1.00	ZINC93145903	0.000	302
	Hydrogen Donor	22.98	-35.00	7.99	0.50	ZINC02426494	0.000	499
	Hydrogen Acceptor	22.98	-35.00	7.99	0.50	ZINC00896463	0.000	293
4	Hydrogen Donor	12.01	-41.85	4.62	0.50	ZINC42117225	0.000	410
	Hydrogen Acceptor	12.01	-41.85	4.62	0.50	ZINC92185901	0.000	356
	Hydrophobic	21.70	-39.32	12.05	1.00	ZINC92093016	0.000	275
5	Hydrogen Donor	12.01	-41.85	4.62	0.50	ZINC16134090	0.036	472
	Hydrophobic	22.04	-38.90	14.75	1.00	ZINC13980125	0.050	475
	Hydrogen Acceptor	22.02	-35.88	5.58	0.50	ZINC00942843	0.050	447

### 3.2.3.3 Molecular Docking Results for TIGIT

The top three molecules with the most negative Gibbs free energies ( $\Delta G$ ) are ZINC00119434 (-10.55 kcal/mol), ZINC11616526 (-10.48 kcal/mol), and ZINC00896463 (-10.32 kcal/mol). Theoretically, these three molecules have a more thermodynamically favorable interaction with TIGIT than the other twelve molecules. The druglikeness and commercial availability of the three molecules will subsequently be explored, and experiments will be performed to examine whether binding and inhibition of TIGIT are successful.

**Table 12.** List of the Lowest Binding Free Energy from Swissdock.

Compound	Cluster	Full Fitness (kcal/mol)	Estimated $\Delta G$ (kcal/mol)
ZINC11616526	2	-2181.93	-10.48
ZINC03794711	0	-2156.03	-9.87
ZINC02901892	0	-2240.06	-7.82
ZINC00119434	1	-2233.92	-10.55

ZINC59187897	27	-2207.16	-7.87
ZINC77591929	10	-2293.13	-8.33
ZINC93145903	1	-2323.51	-7.64
ZINC02426494	2	-2149.08	-7.78
ZINC00896463	5	-2229.31	-10.32
ZINC42117225	2	-2242.78	-7.94
ZINC92185901	1	-2263.11	-7.98
ZINC92093016	8	-2195.08	-7.18
ZINC16134090	0	-2248.67	-8.46
ZINC13980125	17	-2218.49	-8.38
ZINC00942843	5	-2220.70	-7.97

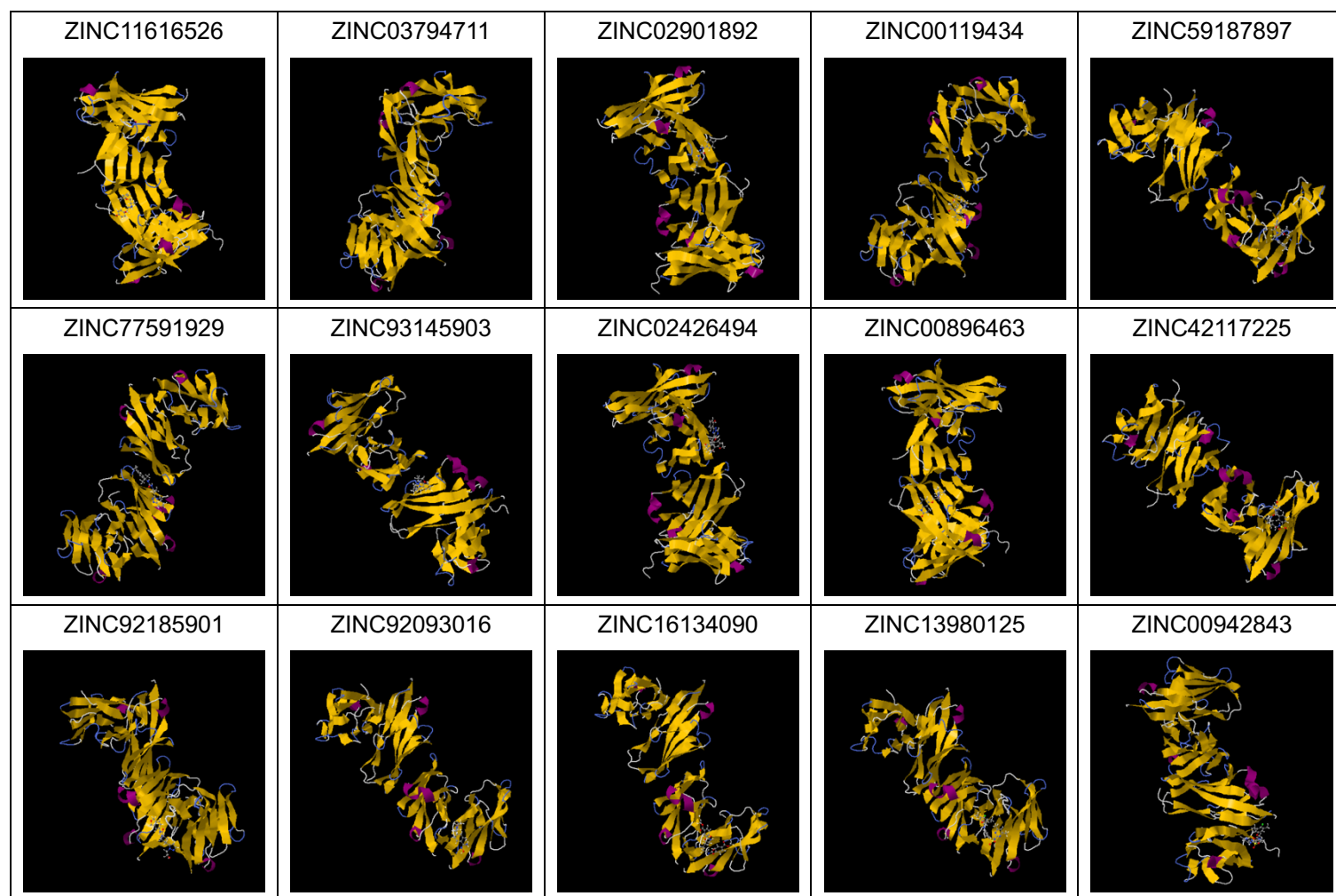


**Figure 13.** Molecular docking results of selected molecules from Swissdock.

#### 3.2.3.4 Drug Properties Estimated by SwissADME

All three molecules (ZINC00119434, ZINC11616526, and ZINC00896463) follow the Lipinski's rule. The three molecules are highly possible for drug utility.

**Table 13.** The druglikeness of the molecules.



	Number of hydrogen bond donors	Calculated LogP value	Molecular mass (g/mol)	Number of hydrogen bond acceptors	Druglikeness according to the Lipinski's rule
ZINC00119434	1	2.78	335.42	2	Yes
ZINC11616526	3	2.65	302.39	3	Yes
ZINC00896463	3	2.58	293.38	3	Yes

### 3.2.3.5 Commercial availability

Among the three molecules, only ZINC00119434 and ZINC00896463 are commercially available. Subsequent experiments are performed using ZINC00119434 and ZINC00896463 as potential inhibitors.

### 3.2.3.6 Detection of Protein-Small Molecule Interaction Using MST

Based on the MST results, the plot of  $F_{\text{norm}}$  against molecule concentration is roughly constant for ZINC00119434 but decreases gradually for ZINC00896463. This indicates that ZINC00896463 binds to TIGIT, while ZINC00119434 does not.

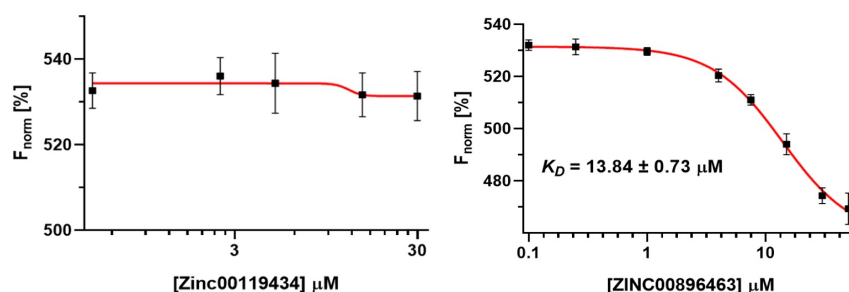


**Figure 14.** Monitoring fluorescence change using MST to assess the TIGIT binding affinity with ZINC00119434 (left) and ZINC00896463 (right).

### 3.2.3.7 Investigation of ZINC67909114 on TIGIT inhibition in a Cell-free Environment

The results from AlphaLISA show that as the two small molecule concentrations increase, only the percent activity for ZINC00896463 decreases. Therefore, ZINC00896463 is the successful inhibitor for the interaction between TIGIT and CD155.

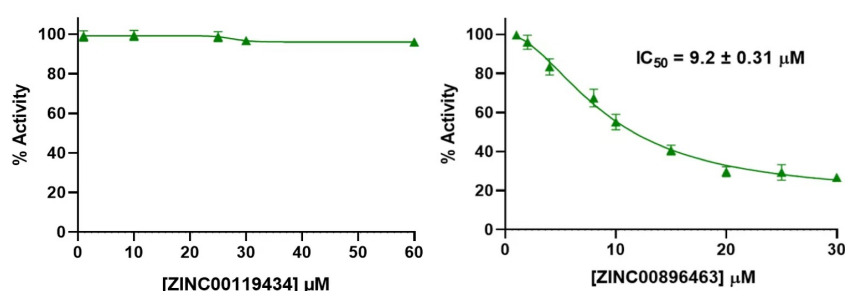


**Figure 15.** Using the change in percent activity from AlphaLISA to evaluate ZINC00119434 (left) inhibition and ZINC00896463 (right) inhibition of TIGIT/CD155 interaction.

### 3.2.3.8 Investigation of ZINC67909114 on TIGIT Inhibition in a Cell-based Environment

In contrast to the AlphaLISA experiment, the Promega blockage bioassay examines the inhibition of ZINC00896463 on TIGIT in a cell-based environment. The bioassay contains two cell types that closely resemble the interaction of cells in the human body. The result shows that the luminescence gradually increases as the concentration of ZINC00896463 increases. When 50  $\mu\text{M}$  of ZINC00896463 is added, the luminescence reaches about 9000 RLU. Therefore, ZINC00896463 is validated to be an effective inhibitor in a cell-based

environment.

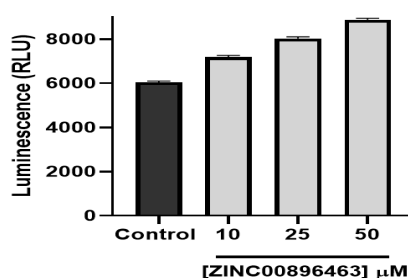


**Figure 16.** Using the change in luminescence signal from the Promega bioassay to evaluate its ability to inhibit TIGIT/CD155 binding in a cell-based assay.

## 4. Future Research

The promising results presented above set the stage for testing the inhibition of ZINC00896463 on TIGIT using an in vivo model. C57BL/6 wild-type (WT) mice (eight- to twelve weeks old) will be used. Mice will be divided into two groups (group A and group B) and subcutaneously (s.c.) injected with  $1 \times 10^6$  MC38 cells or  $2 \times 10^5$  -CT26 cells, respectively, on day zero. On day seven, the mice will be further randomly divided into two groups and intraperitoneal (i.p.) treated with 5 mg/kg of ZINC00896463 or normal saline every day for two weeks. Tumor volume will be measured every other day. All mice will be sacrificed at the end of the treatment (the twenty-second day). Results will be displayed in two plots, each for one tumor cell, showing how the tumor volume changes over time with or without ZINC00896463.

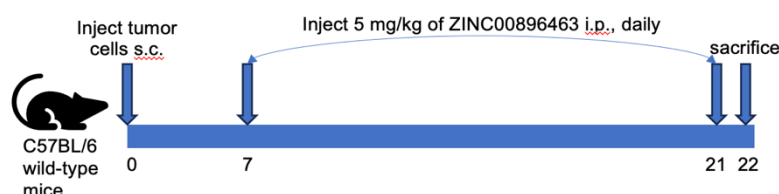


**Figure 17.** Schematic representation of the in vivo model to evaluate ZINC00896463 inhibition on TIGIT.

## 5. Conclusion

In this research, I completed interconnected experiments to search for small molecules useful for TIGIT inhibition. The pharmacophore models of TIGIT/CD112 interaction and TIGIT/CD155 interaction were used for virtual screening to identify potential inhibitors. The molecules with higher matching to the pharmacophore clusters were identified. The energies of interaction between these molecules with TIGIT were then estimated, and the top molecules with a more favorable interaction with TIGIT were selected. The drug properties and commercial availabilities of those small molecules were examined. Lastly, experiments applying MST, AlphaLISA, and the Promega blockage bioassay were performed to validate small molecules' inhibition on TIGIT. At the end of the research, ZINC00896463 was identified and verified as the small molecule that could inhibit TIGIT/CD155 interaction in both cell-free and cell-based assays. Future research will be performed by applying an in vivo experiment to test the influence of ZINC00896463 on tumor growth. If future results are optimistic, ZINC00896463 could serve as a clinical inhibitor for TIGIT, bringing new insights into cancer immunotherapy.

## 6. Acknowledgments

I want to thank my mentor, Dr. Moustafa Gabr, for discussing the research topic, providing valuable suggestions, and giving me feedback on my paper writing. I would also like to thank Dr. Qiang (Steven) Chen, my high school chemistry teacher, for teaching me the fundamental knowledge of chemistry.

## References

1. Roy, P S, and B J Saikia. "Cancer and cure: A critical analysis." *Indian journal of cancer* vol. 53,3 (2016): 441-442.
2. Singh, Poonam. "World Cancer Day: Close the care gap", World Health Organization, 4 February 2023
3. Siegel, Rebecca L et al. "Cancer statistics, 2023." *CA Cancer J Clin.* 73,1 (2023): 17-48.
4. Hausman, Daniel M. "What Is Cancer?." *Perspectives in biology and medicine* vol. 62,4 (2019): 778-784.
5. "Cancer", Newsroom, World Health Organization, <https://www.who.int/news-room/fact-sheets/detail/cancer>
6. "What Is Cancer?", About Cancer, National Cancer Institute, <https://www.cancer.gov/about-cancer/understanding/what-is-cancer>
7. "How can cancer kill you?", About Cancer, Cancer Research UK, <https://www.cancerresearchuk.org/about-cancer/coping/dying-with-cancer/how-can-cancer-kill-you>
8. Wang, J-J et al. "Tumor microenvironment: recent advances in various cancer treatments." *European review for medical and pharmacological sciences* vol. 22,12 (2018): 3855-3864.
9. Baskar, Rajamanickam et al. "Cancer and radiation therapy: current advances and future directions." *International journal of medical sciences* vol. 9,3 (2012): 193-9.
10. Alfouzan AF. Radiation therapy in head and neck cancer. *Saudi Med J.* 2021 Mar;42(3):247-254.
11. Osipov, Arsen et al. "From immune checkpoints to vaccines: The past, present and future of cancer immunotherapy." *Advances in cancer research* vol. 143 (2019): 63-144.
12. Park, Y.J., Kuen, DS. & Chung, Y. Future prospects of immune checkpoint blockade in cancer: from response prediction to overcoming resistance. *Exp Mol Med* 50 (2018): 1–13.
13. Van den Bulk J, Verdegaal EM, de Miranda NF. Cancer immunotherapy: broadening the scope of targetable tumours. *Open Biol.* 2018 Jun;8(6):180037.
14. Tan, Shuzhen et al. "Cancer immunotherapy: Pros, cons and beyond." *Biomedicine & pharmacotherapy = Biomedecine & pharmacotherapie* vol. 124 (2020): 109821.
15. Riley RS, June CH, Langer R, Mitchell MJ. Delivery technologies for cancer immunotherapy. *Nat Rev Drug Discov.* 2019 Mar;18(3):175-196.
16. Abril-Rodriguez G, Ribas A. SnapShot: Immune Checkpoint Inhibitors. *Cancer Cell.* 2017;31(6):848-848.
17. Marin-Acevedo, J.A., Soyano, A.E., Dholaria, B. et al. Cancer immunotherapy beyond immune checkpoint inhibitors. *J Hematol Oncol* 11, 8 (2018).
18. Wilky, Breelyn A. "Immune checkpoint inhibitors: The linchpins of modern immunotherapy." *Immunological reviews* vol. 290,1 (2019): 6-23.
19. Darvin, Pramod et al. "Immune checkpoint inhibitors: recent progress and potential biomarkers." *Experimental & molecular medicine* vol. 50,12 1-11.
20. Yu, X., Harden, K., C Gonzalez, L. et al. The surface protein TIGIT suppresses T cell activation by promoting the generation of mature immunoregulatory dendritic cells. *Nat Immunol* 10 (2009): 48–57
21. Ge, Zhouhong et al. "TIGIT, the Next Step Towards Successful Combination Immune Checkpoint Therapy in Cancer." *Frontiers in immunology* vol. 12 699895. 22 Jul. 2021.
22. Chauvin, Joe-Marc, and Hassane M Zarour. "TIGIT in cancer immunotherapy." *Journal for immunotherapy of cancer* vol. 8,2 (2020): e000957.

23. Harjunpää, H, and C Guillerrey. "TIGIT as an emerging immune checkpoint." *Clinical and experimental immunology* vol. 200,2 (2020): 108-119.
24. Zhang, Q., Bi, J., Zheng, X. et al. Blockade of the checkpoint receptor TIGIT prevents NK cell exhaustion and elicits potent anti-tumor immunity. *Nat Immunol* 19 (2018): 723–732.
25. Volkamer, Andrea et al. "Combining global and local measures for structure-based druggability predictions." *Journal of chemical information and modeling* vol. 52,2 (2012): 360-72.
26. Ngan, Chi-Ho et al. "FTSite: high accuracy detection of ligand binding sites on unbound protein structures." *Bioinformatics (Oxford, England)* vol. 28,2 (2012): 286-7.
27. J Jendele, Lukas et al. "PrankWeb: a web server for ligand binding site prediction and visualization." *Nucleic acids research* vol. 47,W1 (2019): W345-49.
28. Koes, David Ryan, and Carlos J Camacho. "PocketQuery: protein-protein interaction inhibitor starting points from protein-protein interaction structure." *Nucleic acids research* vol. 40,Web Server issue (2012): W387-92.
29. Koes, David Ryan, and Carlos J Camacho. "Small-molecule inhibitor starting points learned from protein-protein interaction inhibitor structure." *Bioinformatics (Oxford, England)* vol. 28,6 (2012): 784-91.
30. Koes, David Ryan, and Carlos J Camacho. "ZINCPharmer: pharmacophore search of the ZINC database." *Nucleic acids research* vol. 40,Web Server issue (2012): W409-14.
31. Grosdidier, Aurélien et al. "SwissDock, a protein-small molecule docking web service based on EADock DSS." *Nucleic acids research* vol. 39,Web Server issue (2011): W270-7.
32. Daina, A., Michielin, O. & Zoete, V. SwissADME: a free web tool to evaluate pharmacokinetics, drug-likeness and medicinal chemistry friendliness of small molecules. *Sci Rep* 7, 42717 (2017).
33. Rasooly, Avraham and Herold, Keith. "Biosensors and Biodetection: Methods and Protocols, Volume 1: Optical-Based Detectors" Humana Press, 3-4
34. *Anal. Chem.* 1990, 62, 18, 950A–959A
35. M. Jerabek-Willemsen et al. "MicroScale Thermophoresis: Interaction analysis and beyond" *J. Mol. Struct.* Volume 1077, 2014, 101-113
36. "AlphaLISA Immunoassays," Life Sciences & Diagnostics, Revvity, <https://www.perkinelmer.com/category/immunoassays-alpha>
37. "Data Sheet TIGIT:CD112 Homogeneous Assay Kit", BPS Bioscience.
38. Yan, Y., Tao, H., He, J. et al. The HDock server for integrated protein–protein docking. *Nat Protoc* 15 (2020): 1829–52.
39. "TIGIT/CD155 Blockade Bioassay", Immune Checkpoint Bioassays, Promega Products, <https://www.promega.com/products/reporter-bioassays/immune-checkpoint-bioassays/tigit-cd155-blockade-bioassay/?catNum=J2201>
40. Deuss, Felix A et al. "Recognition of nectin-2 by the natural killer cell receptor T cell immunoglobulin and ITIM domain (TIGIT)." *The Journal of biological chemistry* vol. 292,27 (2017): 11413-11422.

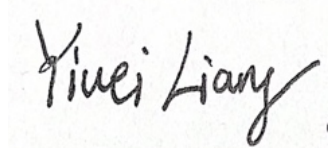
## Declaration of Academic Integrity

The participating team declares that the paper submitted is comprised of original research and results obtained under the guidance of the instructor. To the team's best knowledge, the paper does not contain research results, published or not, from a person who is not a team member, except for the content listed in the references and the acknowledgment. If there is any misinformation, we are willing to take all the related responsibilities.

### **Names of team members:**

Yiwei Liang

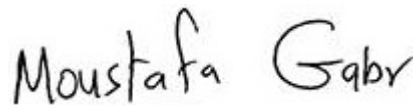
### **Signatures of team members:**

A handwritten signature in black ink that reads "Yiwei Liang". The signature is written in a cursive style with a large, sweeping 'Y' and a long horizontal stroke at the end.

### **Name of the instructor:**

Moustafa Gabr

### **Signature of the instructor:**

A handwritten signature in black ink that reads "Moustafa Gabr". The signature is written in a cursive style with a large, sweeping 'M' and a long horizontal stroke at the end.

Date: August 19<sup>th</sup>, 2023